5

Reconciling Mott-Statistical and Energy-Based Fragmentation

In earlier sections the statistical fragmentation theory of Mott was considered in some depth. An alternative fragmentation theory based on energy balance principals has also been pursued by the present author and others. As posed, the two theories appear to be based on strikingly different principals. In the present section attempts are pursued to understand and reconcile differences between the two theories. For the purpose of this reconciliation the essential features of both theories are summarized. This summary represents a condensation of same the material provided in the previous sections.

The present discussion will focus on the one-dimensional expanding ductile ring fragmentation as originally posed by Mott. To provide an experimental grounding for the theoretical comparisons the dynamic fragmenting ring data on uranium 6% niobium [Grady and Olsen, 2003], discussed in further detail later in this report, is used.

5.1 Mott Statistics-Based Fragmentation

As has been pursued here in some detail, three technical reports published within the first half of 1943 revealed the maturing of Mott's understanding of the dynamic fragmentation process and, in the last of these reports, a statistical theory of fragmentation emerged, which is still one of the leading theories available. The theory was published several years later in the open literature [Mott, 1947]. This development is summarized in the following subsections.

5.1.1 The Mott Cylinder

The Mott theory of fragmentation is most readily conceptualized by again considering the Mott cylinder (or ring) illustrated in Fig. 5.1. The Mott cylinder is an idealization of an expanding cylindrical shell whose outward motion is imparted by some radial impulse. Mott, in particular, focused on the natural fragmentation of exploding pipe bombs. The model is applicable to other

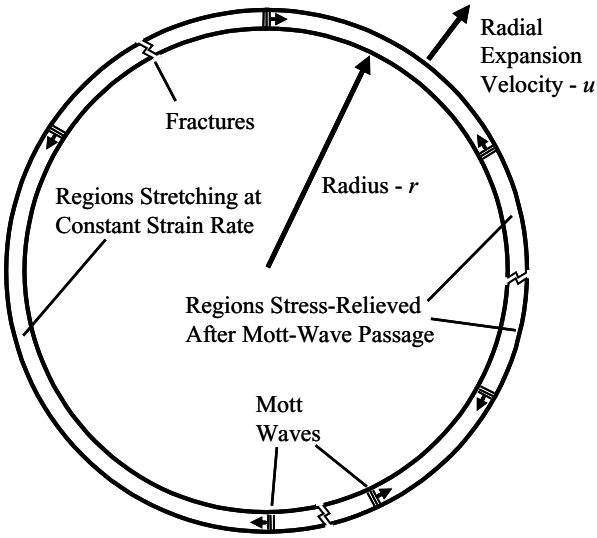

Fig. 5.1. Mott cylinder illustrating the one-dimensional activation and interaction of fractures leading to the statistical fragmentation of the body

test conditions such as the magnetically driven metal ring data considered in the present section.

An explosively-driven expanding metal cylinder is a decidedly multidimensional fragmentation event, and fragmentation of the Mott cylinder is only an approximation to this event. The theory attempts to capture the characteristic circumferential spacing of fractures and the statistical distribution in the spacing. It is not intended to account for the axial propagation and interaction of cracks within a finite length cylinder. The Mott cylinder is an expanding metal body with radial velocity u and radius r at the time when multiple fracture and break up of the cylinder proceeds. Just preceding break up, the cylinder body is in circumferential tension and undergoing uniform circumferential stretching at a rate given by the ratio $\dot{\varepsilon} = u/r$.

Mott proposed that fragmentation proceeded through the random spatial and temporal occurrence of fractures resulting in a distribution in fragment lengths. Release waves propagate away from the sites of fracture relieving the tension and precluding the possibility for further fracture within the regions encompassed by tension release waves. Fragmentation is complete when fracture-induced release waves subsume the entire cylinder.

Thus, within the model for dynamic fragmentation proposed by Mott, two physical issues need to be addressed. First, is the issue of when and where fractures occur on the Mott cylinder. Second, is the nature of propagation of tensile release waves (Mott waves) away from the sites of fracture. Here each issue will be addressed in turn.

5.1.2 Mott Fracture Activation

Mott put forth arguments that energy dissipation was not of consequence in the fracture process and proposed instead a statistical strain-to-fracture criterion. Mott assumed that fractures occurred at random, around the circumference of the cylinder at a frequency governed by a strain dependent hazard function $\lambda(\varepsilon)$ [e.g., Hahn and Shapiro, 1967], such that $\lambda(\varepsilon)d\varepsilon$ provided the statistical number of fractures occurring within a unit length of the cylinder circumference in the strain interval $d\varepsilon$. It is important to recognize that Mott considered $\lambda(\varepsilon)$ to be an independently measurable property of the material. An alternative and complementary application of the hazard function yields,

$$F(\varepsilon) = 1 - e^{-L\int \lambda(\varepsilon)d\varepsilon}, \tag{5.1}$$

for the cumulative probability of fracture failure in tensile test specimens of length L. Mott in fact used tensile test data on steels to estimate parameters in the function $\lambda(\varepsilon)$ as discussed in the preceding section.

Mott expected $\lambda(\varepsilon)$ to be a strongly increasing function of strain and suggested both an exponential and a power-law function. The former leads to Gumbel statistics, while the latter yields Weibull statistics. Relative differences between the two distributions were identified earlier in this report. Mott pursued the exponential hazard function. Here the two-parameter power-law hazard function,

$$\lambda(\varepsilon) = \frac{n}{\sigma}\left(\frac{\varepsilon}{\sigma}\right)^{n-1}, \tag{5.2}$$

will be used. For reasonably large n the parameter σ is the expected value of the strain to fracture of a unit length while σ/n is proportional to the standard deviation in the strain to fracture.

5.1.3 Mott Tension Release

Statistical fracture in the Mott cylinder can now be generally addressed. The tensile release function is,

$$D_x(\varepsilon) = \int_0^{\varepsilon} 2g(\varepsilon - \eta)\lambda(\eta)\, d\eta\,, \tag{5.3}$$

where $\lambda(\eta)d\eta$ is the statistical number of fractures activated on the Mott cylinder at a strain η within interval $d\eta$. The function $g(\varepsilon - \eta)$ is the distance traveled by a tensile stress release wave over the strain interval $\varepsilon - \eta$ for one fracture. (Since strain rate is assumed to be constant over the duration of the fracture process, strain and time are synonymous through $\varepsilon = \dot{\varepsilon}t$.)

In (5.3) $D_x(\varepsilon)$ is seen to provide the fraction of the Mott cylinder which has been encompassed by stress release waves emanating from sites of fracture at a current strain ε. The equation also determines the fraction of the cylinder

in which further fracture is precluded. A form of (5.3) was derived by Mott in the original 1943 report [Mott, 1943] and discussed in the previous several chapters.

An inspection of (5.3) reveals that the function $D_x(\varepsilon)$ will exceed unity at sufficiently large strain. This non-physical result is a consequence of not accounting for two factors in the fracture activation and stress wave propagation process. First, the fracture activation function $\lambda(\varepsilon)$ does not exclude the activation of further fractures within regions previously stress relieved. Second, the stress release function $g(\varepsilon)$ does not account for the impingement and the overlap of opposing release waves from separate neighboring fractures. Thus, (5.3) is only applicable for a dilute number of fractures early in the fracture and release process.

To account for fracture exclusion and wave impingement in the statistically random Mott model, a statistical method introduced by Johnson and Mehl (1939) discussed in the previous chapter is used. Exclusion and impingement is accounted for through the relation,

$$D(\varepsilon) = 1 - e^{-D_x(\varepsilon)} \,, \tag{5.4}$$

providing the fraction of the Mott cylinder $D(\varepsilon)$ encompassed by fracture stress release waves at any strain ε. $D(\varepsilon)$ and $D_x(\varepsilon)$ are equivalent at early times as they should be. The function $D(\varepsilon)$ does approach unity as ε becomes large.

5.1.4 Fracture Stress Release Function

A functional form of the stress release function $g(\varepsilon)$ must be specified. There are several possibilities. If the expanding Mott cylinder is elastic at the time of fracture, then a constant elastic release wave velocity governed by the elastic modulus is sensible. Mott, however, considered an expanding ductile metal cylinder and assumed a material on the tensile yield surface governed by a constant flow stress Y. Instantaneous fracture and rigid-ideally-plastic constitutive response leads to the stress release function,

$$g(\varepsilon) = \sqrt{\frac{2Y}{\rho \dot{\varepsilon}^2} \varepsilon} \,. \tag{5.5}$$

It was shown earlier that diffusion rather than wave propagation governs stress release under the assumed physical conditions.

5.1.5 Fracture Number Prediction

Given explicit forms for the fracture activation function from (5.2) and the stress release function from (5.5), statistical predictions of the number of fractures (and fragments) produced in the break-up of the Mott cylinder can be

determined. Accounting for the stress relieved fraction of the cylinder $D(\varepsilon)$, the number of fractures at a strain ε is given by,

$$N(\varepsilon) = \int_0^{\varepsilon} (1 - D(\eta))\lambda(\eta)\, d\eta \; . \tag{5.6}$$

Completing the integral in (5.3) and using (5.4) to obtain $D(\varepsilon)$, integration of (5.6) to infinite strain yields,

$$N = \beta_n \left(\frac{\rho \dot{\varepsilon}^2}{2\pi Y} \frac{n}{\sigma} \right)^{n/(2n+1)} \quad , \tag{5.7}$$

for the number of fractures per unit length, where the numerical constant is,

$$\beta_n = \left(\frac{2n}{2n+1} \right)^{1/(2n+1)} \left(\frac{1}{\sqrt{n}} \frac{\Gamma\left(n + 1/2\right)}{\Gamma\left(n\right)} \right)^{2n/(2n+1)} \Gamma\left(\frac{2n}{2n+1} \right) \; . \tag{5.8}$$

For reasonably large n the constant β_n approaches one in (5.7) and the power approaches one-half, leading to a linear dependence of fracture number on the expansion strain rate. The fracture number is determined by the standard deviation ($\simeq 1.283\, \sigma/n$) of the power-law fracture frequency function $\lambda(\varepsilon)$ as was noted by Mott. The statistical temporal history of fractures appearing on the Mott cylinder can be determined by retaining the strain dependence of the integral in (5.6).

5.1.6 Fracture Distribution Prediction

Additionally, the random placement of fractures on the Mott cylinder both in space and in time, as assumed in the Mott model, allows for calculation of the statistical distribution of fracture spacing (fragment lengths). This calculation was performed graphically by Mott and has been completed by analytic methods as shown in the previous section for the special case of $n = 1$ in the power-law fracture frequency function. The calculated analytic distribution in fracture spacing by this analytic method is,

$$f\left(x\right) = \frac{\beta^2}{4} \frac{1}{x_o} \left(\frac{x}{x_o} \right)^3 e^{-\frac{1}{4}(x/x_o)^3} \int_0^1 \left(1 - y^2\right) e^{-\frac{3}{4}(x/x_o)^3 y^2} dy \; , \tag{5.9}$$

where $\beta = 3\Gamma(2/3)$ and $x_o = (3\sigma Y/2\rho\dot{\varepsilon}^2)^{1/3}$. The sensitivity of the size distribution to the functional form of the fracture frequency function $\lambda(\varepsilon)$ is not known, but comparison of the analytic distribution from (5.9) and the graphical distribution of Mott suggests that this sensitivity is probably small. Both the analytic and the graphical distribution are again compared in Fig. 5.2.

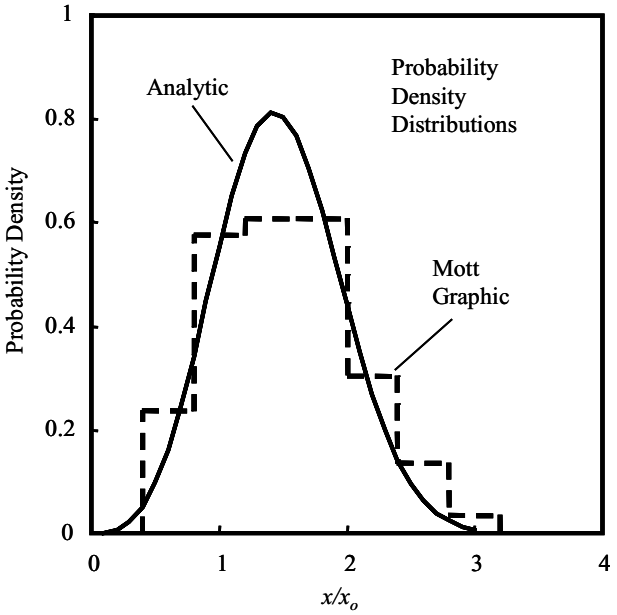

Fig. 5.2. Comparison of the graphic and the analytic solution for the Mott distribution of fragment lengths

In summary, the statistics-based theory of dynamic fragmentation developed in the seminal study of Mott provides a physically plausible and intellectually satisfying description of the fragmentation process. Within the one-dimensional model of the Mott cylinder the theory is fully predictive, providing the average fragment size and the distribution about the average, as well as the statistical temporal history of fracture and the strain-to-fracture.

5.2 Energy-Based Fragmentation

A theory of dynamic fragmentation based on markedly different initial assumptions has also been pursued [Grady et al., 1984; Kipp and Grady, 1985]. Again, the one-dimensional fracture and fragmentation on the Mott cylinder in Fig. 5.1 provides the model for consideration of the theory in the present context. The fundamental difference in the two theories is that Mott assumed energy dissipated in the fracture process was not of concern, and that fracture at a site on the cylinder would be effectively instantaneous. In contrast, energy dissipation and an associated fracture delay time lies at the heart of the energy-based fragmentation theory.

5.2.1 Fracture Calculation

Formulation of the energy-based fragmentation theory on the expanding ductile Mott cylinder proceeds by extending the stress release analysis developed by Mott to calculate the time history of plastic release waves (Mott waves) emanating from sites of fracture. The extension of the analysis has been pursued in Chaps. 3 and 4, and proceeds by considering, rather than instantaneous fracture, a fracture resistance which reduces from the flow stress Y to zero as a crack-opening-displacement parameter y goes from zero to some critical crack opening displacement y_c. An assumption of linear reduction of the fracture resistance then leads to a fracture energy dissipation $\Gamma = Y y_c/2$. The assumption of other functional forms for the reduction of fracture resistance (Chap. 4) does not markedly alter the value of Γ. Momentum balance for the rigid ideally plastic problem leads to the following differential expression for the position x of the Mott release wave [Kipp and Grady, 1985],

$$\rho\dot{\varepsilon}x\frac{dx}{dt} = \frac{Y^2}{2\Gamma}y \ , \tag{5.10}$$

while motion of the crack opening displacement gives,

$$\frac{dy}{dt} = \dot{\varepsilon}x \ . \tag{5.11}$$

The coupled equations are readily solved yielding,

$$x(t) = \frac{1}{12}\frac{Y^2}{\rho\Gamma}t^2 \ , \tag{5.12}$$

for the motion of the Mott release wave while crack opening over $0 \leq y \leq y_c$ is given by,

$$y(t) = \frac{1}{36}\frac{\dot{\varepsilon}Y^2}{\rho\Gamma}t^3 \ . \tag{5.13}$$

The time to fracture is determined by the time for the crack opening displacement to achieve y_c and is calculated to be,

$$t_c = \left(\frac{72\rho\Gamma^2}{Y^3\dot{\varepsilon}}\right)^{1/3} \ . \tag{5.14}$$

Over the time t_c the Mott release wave travels a distance from the site of fracture,

$$x_c = \left(\frac{3\Gamma}{\rho\dot{\varepsilon}^2}\right)^{1/3} \ . \tag{5.15}$$

5.2.2 Fragment Size and Fragmentation Toughness

The distance x_c over which the Mott release wave propagates determines the minimum spacing of separate fractures permitting fracture completion without interaction of release waves. The theory assumes that the nominal fragment length x_o is given by twice the distance x_c or,

$$x_o = 2x_c = \left(\frac{24\Gamma}{\rho\dot{\varepsilon}^2}\right)^{1/3} . \tag{5.16}$$

The fracture resistance Γ is considered to be a property of the material characterizing the dissipation in the fracture growth process. It is possible, under certain failure modes, to estimate the fracture resistance Γ from other material properties [Kipp and Grady, 1985]. Fracture toughness is the property commonly used to quantify the static (and dynamic) fracture resistance of metals. Thus, it is sensible in the present development to define a property with the dimensions of fracture toughness through the relation of linear elastic fracture mechanics relating fracture strain energy release and fracture toughness. Namely,

$$K_f = \sqrt{2E\Gamma} , \tag{5.17}$$

where E is the elastic modulus. The property K_f will be identified as the fragmentation toughness of the metal and will not presume any relationship to the clearly defined static fracture toughness K_c. Frequently, however, K_c is found to provide a very adequate first order estimate for the fragmentation toughness as will be shown in later chapters. The expression for the characteristic fracture spacing from (5.16) then becomes,

$$x_o = \left(\frac{\sqrt{12}K_f}{\rho c\dot{\varepsilon}}\right)^{2/3} . \tag{5.18}$$

The energy-based theory does not address the issue of the statistical distribution of fragment sizes. It is assumed that (5.18) provides an average fragment size and that the fragment number per unit length is provided by the inverse of (5.18), or,

$$N = \left(\frac{\rho c\dot{\varepsilon}}{\sqrt{12}K_f}\right)^{2/3} . \tag{5.19}$$

Thus, (5.19) provides the energy-based spatial fracture frequency prediction to be compared with (5.7) of the Mott statistical theory.

5.3 Comparisons of the Fragmentation Theories with Experiment

A range of diverse experimental fragmentation investigations could be used, and in fact has been used, to explore the predictive abilities of Mott's

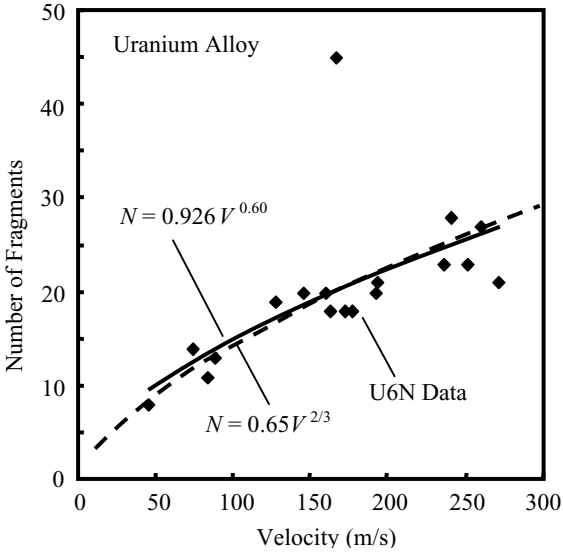

Fig. 5.3. Fragment number versus expansion velocity at fracture for U6Nb expanding ring fragmentation tests

statistics-based theory and the more recent energy-based fragmentation theory. Here, consideration will be restricted to a recent quite-thorough study of dynamic fragmentation of magnetically driven uranium-6%-niobium (U6Nb) metal rings with pertinent experimental data shown in Figs. 5.3 and 5.4. Further details on the experimental test method are provided in a later chapter. The experimental geometry nicely replicates the fragmentation model assumed by Mott and provides data directly comparable with the theoretical predictions.

5.3.1 Experimental Fragmentation Results

In the selected study U6Nb metal rings approximately 30 mm in diameter and with a 0.75 mm square cross section were accelerated by a pulsed magnetic field to radial velocities in the range of 50–300 m/s. Actual acceleration is provided by an aluminum pusher ring which accommodates most of the induced electric current. The aluminum ring is arrested prior to fragmentation allowing free flight of the U6Nb ring preceding break up. Additional details are provided in Chap. 8.

Radial velocity history of the U6Nb rings was measured with time-resolved velocity interferometry or VISAR [Barker and Hollenbach, 1972]. Measured deceleration of the freely expanding ring prior to fragmentation was used to calculate a tensile flow stress of nominally one GPa for the selected heat treated material. Fragmentation for the corresponding material occurred at an expansion of approximately 30%.

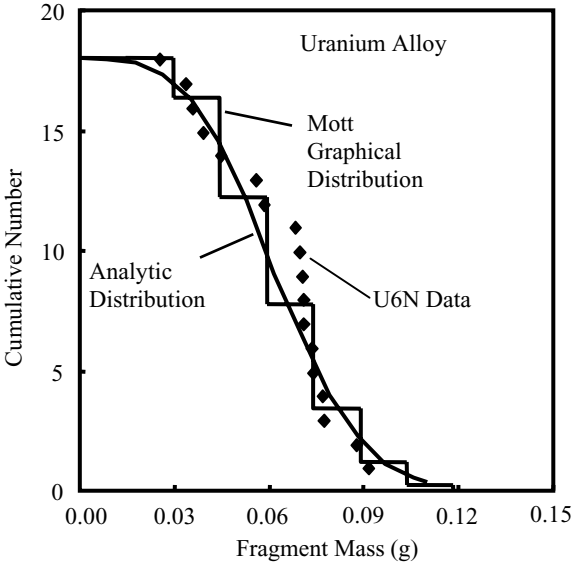

Fig. 5.4. Comparison of cumulative fragment distribution for one representative U6Nb expanding ring fragmentation test with the theoretical Mott fragment size distribution

In each test the number of fragments produced (equivalently, the number of fractures) was determined. Fragment number versus the expansion velocity at fragmentation are shown for the series of U6Nb expanding ring experiments in Fig. 5.3. The anomalous point high on the graph is the consequence of one test on a markedly differently heat treated U6Nb sample (discussed further in Chap. 8). A least squares fit, excluding the one anomalous point, provided the power law representation of the data shown in Fig. 5.3. In one representative test each fragment was separately weighed and the complementary cumulative fragment size distribution shown in Fig. 5.4 was obtained.

5.3.2 Comparison with the Mott Statistics-Based Theory

Weibull parameters σ and n are necessary in the Mott statistical theory to predict the fragment number dependence on velocity (or strain rate) and are not available for the U6Nb material tested. Hence, only sensibility of the experimental results can be examined. The observed experimental power law dependence of fragment number on expansion velocity is close to two-thirds and indicates that the Weibull parameter n in (5.7) is very close to unity. Assuming that $n = 1$, the second Weibull parameter is calculated to be $\sigma = 7.7 \times 10^{-5}$m. The standard deviation in strain to fracture calculated from (5.1) is approximately σ/L. Considering specimens of length one centimeter, the nominal length of fragments in the ring tests, a scatter in strain to fracture

of approximately 0.01 or about 3% of the observed 0.30 strain to fracture is calculated. Thus, the Weibull parameters within the Mott statistical theory for the fragmentation of U6Nb rings are quite plausible.

Prediction of the distribution in fracture spacing is also a facet of Mott's statistical theory. Comparison of both the graphic distribution generated by Mott and the analytic distribution from (5.9), both displayed in Fig. 5.2, are compared with the distribution determined experimentally in Fig. 5.4. The observed distribution and the theoretical distributions based on the Mott statistical fracture theory are also in reasonable accord.

5.3.3 Comparison with the Energy-Based Theory

The energy-based fragmentation theory directly predicts from (5.19) a two-thirds power dependence of fragment number on strain rate or, equivalently, the expansion velocity at fracture. A two-thirds power dependence curve is compared with the data and the experimental fit in Fig. 5.3 and shows sensible agreement with the data.

To further test the energy-based theory the fragmentation toughness is calculated through (5.19) for each experiment. This representation is shown in Fig. 5.5. A value of K_f in excess of $60\,\mathrm{MPa{\cdot}m^{1/2}}$ determined from the fragmentation data is remarkably close to a static fracture toughness of approximately 90–110 $\mathrm{MPa{\cdot}m^{1/2}}$ measured on similar U6Nb alloys.

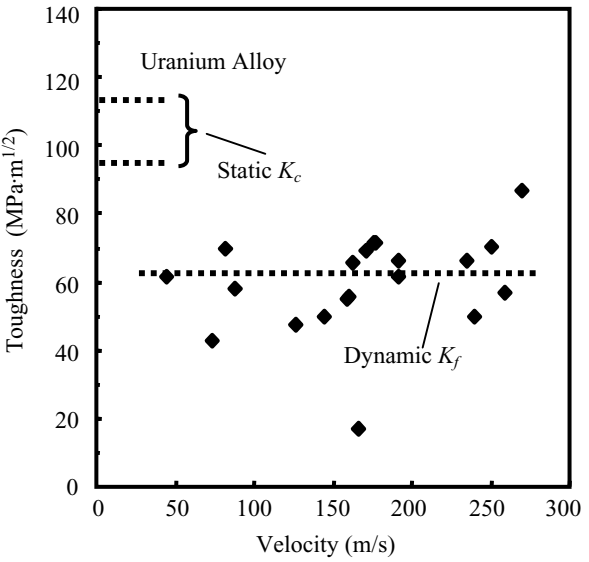

Fig. 5.5. Dynamic fragmentation toughness calculated through theoretical relation relating fragment number, expansion rate and material toughness. Comparison with static toughness data for U6Nb

Other features observed in the U6Nb ring fragmentation experiments also attest to the importance of energy dissipation and finite fracture time in the dynamic fracture process. Inspection of fragments revealed fully developed necking regions – a signature of fractures which were enveloped with tensile release (Mott) waves and fracture growth arrested before full fracture and separation was achieved.

5.3.4 Comments on the Mott Fracture Frequency Function

In the development of the Mott statistical fragmentation theory a statistical fracture frequency function was required. Mott discussed two very viable functional forms; the power law,

$$\lambda(\varepsilon) = \frac{n}{\sigma}\left(\frac{\varepsilon}{\sigma}\right)^{n-1} , \tag{5.20}$$

and the exponential law,

$$\lambda(\varepsilon) = Ae^{\gamma\varepsilon} . \tag{5.21}$$

The latter equation, written in a more common statistical form is,

$$\lambda\left(\varepsilon\right) = \frac{1}{\sigma}e^{(\varepsilon-\mu)/\sigma} , \tag{5.22}$$

where the correspondence to the Mott parameters, introduced in Chap. 3, $\sigma = 1/\gamma$ and $A = (1/\sigma)\exp(-\mu/\sigma)$, is made.

The power law leads to the Weibull extreme value cumulative probability of fracture function,

$$F\left(\varepsilon\right) = 1 - e^{-(\varepsilon/\sigma)^n} , \tag{5.23}$$

and probability density function,

$$f\left(\varepsilon\right) = \frac{n}{\sigma}\left(\frac{\varepsilon}{\sigma}\right)^{n-1} e^{-(\varepsilon/\sigma)^n} . \tag{5.24}$$

Correspondingly, the exponential law,

$$\lambda\left(\varepsilon\right) = \frac{1}{\sigma}e^{(\varepsilon-\mu)/\sigma}, \tag{5.25}$$

provides a Gumbel cumulative probability,

$$F(\varepsilon) = 1 - \exp\left(-e^{(1/\sigma)(\varepsilon-\mu)}\right) , \tag{5.26}$$

and probability density function,

$$f\left(\varepsilon\right) = \frac{1}{\sigma}\exp\left(\frac{1}{\sigma}\left(\varepsilon-\mu\right) - e^{(1/\sigma)(\varepsilon-\mu)}\right) . \tag{5.27}$$

Although, both extreme value representations of the statistical fracture frequency have two parameters, they are far from equivalent. The parameter σ in both is the distribution scale parameter. The Weibull representation also has a distribution shape parameter n, whereas the Gumbel distribution, in contrast, is lacking a shape parameter, but specifies instead the distribution location parameter μ. The Mott fragment number prediction based on a Gumbel fracture frequency representation is,

$$N = \frac{1}{\sqrt{\pi}} \sqrt{\frac{\rho \dot{\varepsilon}^2}{2Y\sigma}} \, . \tag{5.28}$$

The location parameter μ plays no role in the fragment number prediction either in terms of the fragment length scale or in the strain rate dependence. The parameter μ does govern the strain to fracture, however.

The fragment number prediction based on a Weibull representation is,

$$N = \beta_n \left(\frac{\rho \dot{\varepsilon}^2}{2\pi Y} \frac{n}{\sigma} \right)^{n/(2n+1)} , \tag{5.29}$$

and it is observed that the fragment number depends on both the distribution scale and shape parameter.

A location parameter could also be included in the power law fracture frequency and Weibull fracture probability by the replacement $\varepsilon \rightarrow \varepsilon - \mu$. The resulting distribution would then be a three parameter representation. Again, however, the location parameter would control only the strain to fracture and would not influence either the fragment length scale or the strain rate dependence. Equation (5.29) would remain the same.

As the shape parameter n in the Weibull distribution becomes large, the character of the two extreme value distributions becomes similar. The fragment number becomes dependent on the strain rate to the first power in both cases and the fragment size scale is determined solely by the distribution standard deviation (proportional to σ in both cases). As the standard deviation approaches zero both density distributions uniformly converge to a Dirac delta function.

Experimental data, however, suggest a two-thirds power strain rate dependence of fragment number in some cases (although not all). The U6Nb fragmenting ring data discussed here, for example, certainly supports such strain rate dependence. The Weibull fracture frequency representation (with shape parameter $n = 1$) supports this experimental observation. The Gumbel distribution does not.

5.4 Statistical and Energy-Based Theory of Fragmentation

Both Mott's statistical theory and the energy-based theory have features in accord with the results of the U6Nb expanding ring fragmentation experiments.

Frequency, and in particular, the statistical spread in spacing of fractures are consistent with predictions of the Mott theory. The favorable strain rate dependence and the very close agreement between static fracture toughness and the inferred dynamic toughness are, on the other hand, supportive of the energy-based theory. It would seem that a broader theory encompassing concepts from both the statistics-based and the energy-based approaches would be appropriate.

5.4.1 Merging of Theories

The statistical fragmentation theory of Mott is based on two functional properties characterizing response of the material in a dynamic fragmentation event. First, is a strain-dependent fracture activation function $\lambda(\varepsilon)$, which has been selected here as the power law form,

$$\lambda(\varepsilon) = \frac{n}{\sigma}\left(\frac{\varepsilon}{\sigma}\right)^{n-1} . \tag{5.30}$$

Second, is the diffusion-governed tensile stress release propagation function from sites of fracture,

$$g(\varepsilon) = \sqrt{\frac{2Y}{\rho\dot{\varepsilon}^2}\varepsilon} . \tag{5.31}$$

Together the Mott theory yields the spatial fracture frequency from (5.7),

$$N = \beta_n \left(\frac{\rho\dot{\varepsilon}^2}{2\pi Y}\frac{n}{\sigma}\right)^{n/(2n+1)} . \tag{5.32}$$

In contrast, the energy-based theory yields for the average spatial fracture frequency,

$$N = \left(\frac{\rho\dot{\varepsilon}^2}{24\Gamma}\right)^{1/3} . \tag{5.33}$$

The theories are equivalent, if the Weibull constants have the unique values,

$$n = 1 , \tag{5.34}$$

and,

$$\sigma = \beta_1^3 \frac{12}{\pi}\frac{\Gamma}{Y} \cong 5\frac{\Gamma}{Y} . \tag{5.35}$$

Thus, the requisites of the energy theory would uniquely constrain the Weibull parameters and the functional form of the fracture activation function of Mott's statistical theory. Equation (5.35) identifies a material-specific length scale σ and requires, through (5.30), that the fracture activation function be constrained to a constant $\lambda(\varepsilon) = \lambda_o = \sigma^{-1}$.

The fracture activation functions proposed by Mott, and as constrained by the energy theory, are illustrated in Figs. 5.6 and 5.7. The function $\lambda(\varepsilon)$ in

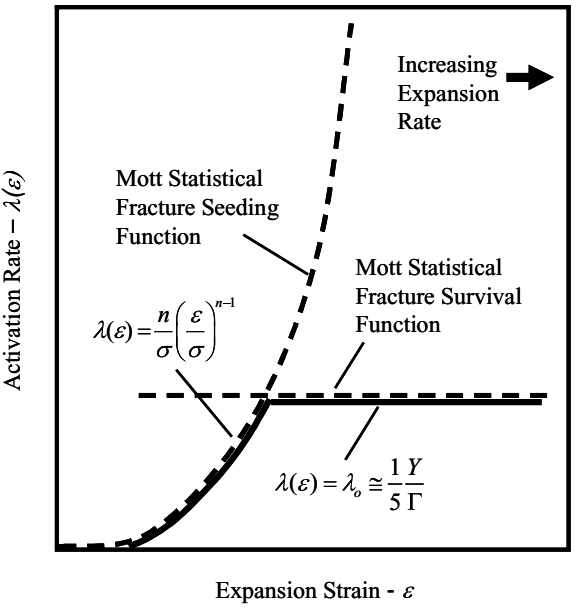

Fig. 5.6. Graphical interpretation of fracture functions in the merging of Mott statistics-based and energy-based fragmentation theories

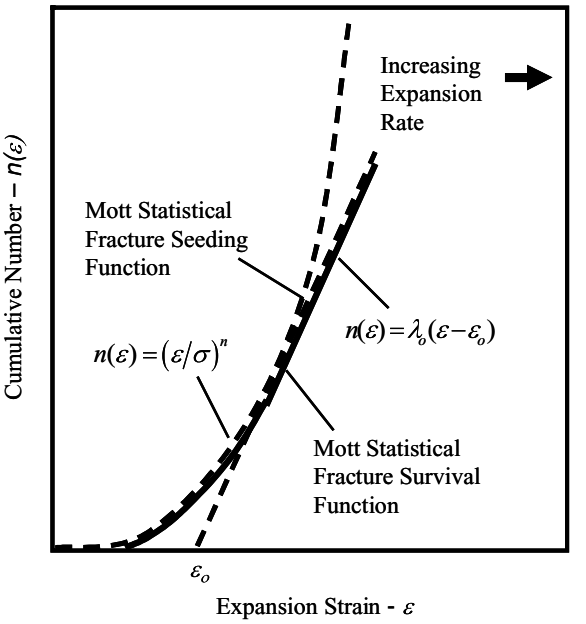

Fig. 5.7. Cumulative fracture seeding and survival functions in statistical energy-based theory of fragmentation

Fig. 5.6 specifies fracture activation frequency as increasing plastic strain ε is achieved. Thus, increasing expansion rates are required to achieve increasing levels of strain to fracture. Below the strain at which the two functions cross in Fig. 5.6, the lower rate of fracture activation is provided by the rapidly increasing power-law expression for $\lambda(\varepsilon)$. Above the cross-over strain the constant expression for $\lambda(\varepsilon) = \lambda_o$, inferred from energy considerations, provides the lesser rate of fracture activation.

From the Mott statistical development outlined earlier, the cumulative strain to fracture is calculated from the expression,

$$\varepsilon_f = \int_0^\infty (1 - D) d\eta \, . \tag{5.36}$$

It is readily shown that the cumulative strain to fracture is $\varepsilon_f = \alpha_n \dot{\varepsilon}^{2/(2n+1)}$ where α_n is a constant function of the material properties. The strain ε_f increases with the expansion rate $\dot{\varepsilon}$. Thus, the comparison indicates that, with increasing expansion rate, a strain to fracture which exceeds the cross-over strain is eventually achieved. Fragmentation and the frequency of fractures become governed by fracture energy dissipation properties above the cross-over strain.

This observation suggests a reinterpretation of the fracture activation functions. The rapidly increasing Mott power law function would, more appropriately, be the fracture seeding function. This function characterizes the perturbations and defects in the body leading to fracture (the seeds of fracture), but does not necessarily specify the fracture activation process itself. Above the cross-over strain the constant energy-based function provides the fracture survival rate. Below the cross-over strain the fracture seeding function limits the fracture activation and there is a one-to-one correspondence between fractures seeded and fractures that survive. Above the cross-over strain, however, many fractures are initiated, but energy requirements limit fracture survival and only a subset of fractures seeded achieve completion.

5.4.2 Strain to Fracture

In the statistical theory of Mott, both strain to fracture and fracture frequency are uniquely determined through the parameters σ and n in the power-law fracture activation function. The theory of Mott, however, cannot also account for the two-thirds power dependence of the average fragment number on strain rate predicted by the energy-based theory, and also observed in the U6Nb expanding ring experiments.

With the extended statistical energy-based theory, strain to fracture in addition to the statistical fragment size and strain-rate dependence features can be accounted for. Prediction is dependent on proper selection of the Mott fracture seeding function,

$$\lambda(\varepsilon) = \frac{n}{\sigma}\left(\frac{\varepsilon}{\sigma}\right)^{n-1} , \tag{5.37}$$

and the energy governed fracture survival function,

$$\lambda(\varepsilon) = \lambda_o , \tag{5.38}$$

where, λ_o has the unique material dependence specified in (5.35). The cumulative number $n(\varepsilon)$, or integral of the fracture seeding and fracture survival functions (the integral of (5.37) and (5.38)), are plotted in Fig. 5.7 (compare with Fig. 5.6). The new parameter revealed in Fig. 5.7 is the constant of integration ε_o of the fracture survival function. The Mott fracture function is determined by the solid segments of both of the functions shown in Fig. 5.7.

The theory has acquired an additional material parameter, but now supports the prediction of strain to fracture in addition to the statistical fracture frequency, spacing distribution, and associated strain-rate dependence. At fracture strain rates into the energy-governed fragmentation regime it is readily shown that the statistical strain to fracture from (5.36) is,

$$\varepsilon_f = \varepsilon_o + \alpha_1 \dot{\varepsilon}^{2/3} , \tag{5.39}$$

where, α_1 is calculated through (5.36) from the energy-based Mott fracture properties. Experimental support for a strain rate dependence of the strain to fracture is presented in Chap. 8.

This broader interpretation of fragmentation merges both the statistical principals of Mott and the fracture energy requirements of the energy-based theory. A wider set of properties characterizing the solid body of interest is required, however. The Mott seeding function characterizes the defect state of the body governing the strain-dependent nucleation of potential fractures. Weibull parameters in the two-parameter power law function serve this purpose in the present development. The Mott survival function incorporates the energy dissipation, or fragmentation toughness, properties of the material. Further material properties and supporting theory are needed to establish onset of the strain to fracture.

5.5 Computational Simulations of Ring Fragmentation

Partial support for the extended theory is provided by a one-dimensional computational simulation of the Mott fragmentation process performed by Kipp and Grady (1986). At that time it was recognized that interplay between dynamics of the fragmentation event and the population of flaws seeding the multiple fracture process could lead to conditions in which flaw structure controlled the extent of fragmentation on one hand while energy limitations controlled fragmentation on the other. A rationale for analytically merging the range of behaviors was not recognized, however.

The following computer simulations of dynamic fragmentation were performed to support experimental fragmenting ring studies performed at that time [Grady et al., 1984]. A one-dimensional finite difference wave code was used to calculate the response of an aluminum rod or wire 0.1 m in length and 1.0 mm in diameter stretching plastically at a flow stress $Y = 100$ MPa and at a uniform stretching rate $\dot{\varepsilon} = 10^4/\text{s}$. Fracture sites were introduced randomly in time according to a constant nucleation rate parameter $\lambda(\varepsilon) = \lambda_o$, and randomly placed within the length of the rod. The nucleation rate λ_o was the only parameter varied over the series of calculations. When fracture was nucleated at a computational cell, stress in that cell was relaxed from the flow stress Y to zero as the cell distended, such that the plastic fracture energy within that cell of $\Gamma = 20\,\text{kJ/m}^2$ was dissipated. The number of fragments produced as the nucleation rate λ_o was varied over approximately one order of magnitude was determined from the simulations and are shown in Fig. 5.8. Although, not directly duplicating the conditions of Fig. 5.7, the relationship is apparent.

At reduced nucleation rates every fracture nucleation site grows to full fracture. The number of fractures and the corresponding characteristic fragment size is, thus, governed fully by the flaw structure and the fracture nucleation (seeding) function. As the nucleation rate is increased the number of nucleated fracture sites which fail to grow to completion correspondingly increases. At

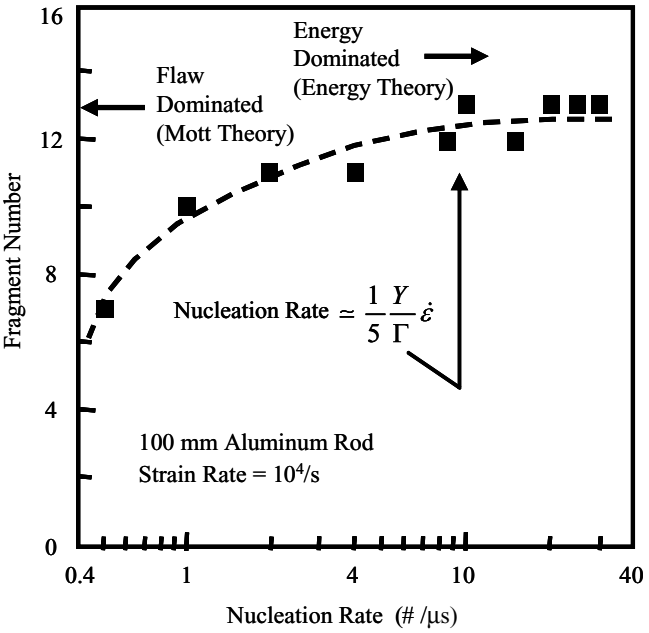

Fig. 5.8. Fragment number from computational simulations of a uniformly stretching aluminum rod [Kipp and Grady, 1986]

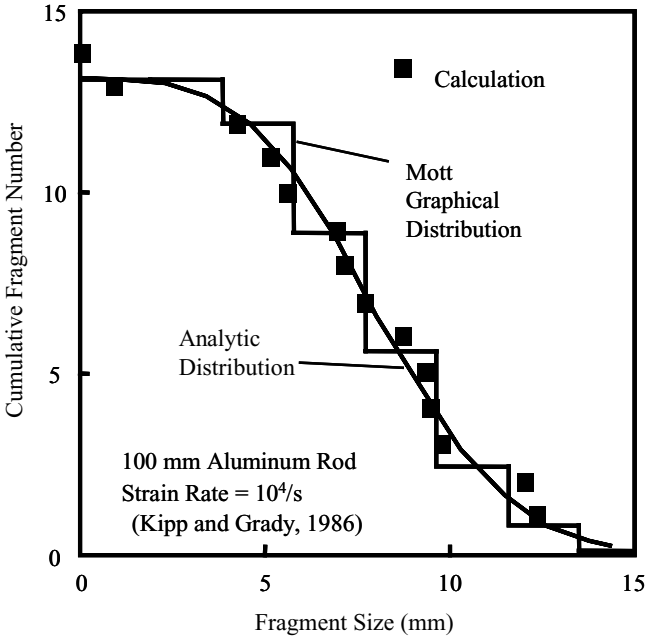

Fig. 5.9. Fragment distribution from computational simulation and comparisons with Mott statistical fragmentation theory

the highest nucleation rates the number of fragments becomes independent of the number of fracture sites nucleated and is determined strictly by the fracture energy Γ resisting fracture growth. The energy governed constant fracture survival rate, $\lambda_o \cong Y\dot{\varepsilon}/5\Gamma$, identified in Fig. 5.8, is sensibly consistent with the expected transition from flaw limited to energy-limited fragmentation.

A cumulative fragment length distribution from one computational simulation is compared with the predicted graphic and analytic Mott distribution in Fig. 5.9. The computational distribution is also fully consistent with the statistical theory.

5.6 Fracture Physics

Of the properties required to characterize the fragmentation response of an expanding metal cylinder, the fracture energy captured through the property Γ is probably the most apparent. That some degree of work must be expended, and some fracture energy overcome, in opening the cracks delineating the fragment boundaries produced in the fragmentation event is inherently reasonable. Less apparent are details of the deformation mechanisms occurring in the fracture growth and dissipation process. Plastic necking, adiabatic

shearing, and ductile fracture are all viable mechanisms. It is likely that all of the above mentioned mechanisms will contribute to some degree.

Considerably less intuitive are the material features responsible for onset of fracture; analytically expressed in this development by the Mott seeding function and quantified by the Weibull parameters in the power-law hazard function. In most events leading to the dynamic expansion and fragmentation of ductile metal rings and shells a degree of stable plastic stretching is accommodated before the fracture occurs. This deformation is most likely a consequence of stabilizing plastic hardening of the component metal. As plastic hardening saturates, however, continued stretching and thinning becomes inherently unstable and susceptible to perturbations in the deformation. Sources of these perturbations are far from certain. Granularity of the device metal is a reasonable source of deformation perturbations. Perturbations from metal granularity leading to fracture would suggest sensitivity of the fragmentation process (particularly the effective strain to fracture) to grain size and related material issues.

There are also convincing indications that surface features, either inherent or induced, play a role in the perturbations seeding fracture onset. Imperfections in metal-explosive interfaces leading to deformation perturbation as detonation-induced shock waves are coupled into the metal system are also suspect.

References

Barker, L. M. and Hollenbach, R. E. (1972), Velocity Interferometer for Measuring the Velocity of any Reflecting Surface, *J. Appl. Phys.*, 43, 4669–4680.

Grady, D. E. and Olsen, M. L. (2003), A Statistical and Energy Based Theory of Dynamic Fragmentation, *Int. J. Eng. Mech.*, 29, 293–306.

Grady, D. E., Kipp, M. E., and Benson, D. A. (1984), Energy and Statistical Effects in the Dynamic Fragmentation of Metal Rings, *Proceedings of the Conference of the Mechanical Properties of High Rates of Strain*, Oxford, 1984, Inst. Phys. Conf. Ser. No. 70, 315–320.

Hahn, G. J. and Shapiro, S. S. (1967), *Statistical Models in Engineering*, John Wiley & Sons, New York.

Johnson, W. A. and Mehl, R. F. (1939), Reaction Kinetics in Processes of Nucleation and Growth, *Trans. AIMME*, 135, 414–458.

Kipp, M. E. and Grady, D. E. (1985), Dynamic Fracture Growth and Interaction in One Dimension, *J. Mech. Phys. Solids* 33 (4), 399–415.

Kipp, M. E. and Grady, D. E. (1986), Random Flaw Nucleation and Interaction in One Dimension, *in Metallurgical Applications of Shock-Wave and High-Strain-Rate Phenomena*, L.E. Murr, K.P. Staudhammer, and M.A. Meyers, eds., Marcel Dekker, Inc., 781–791.

Mott, N. F. (1943), A Theory of the Fragmentation of Shells and Bombs, *Ministry of Supply* AC4035, May.

Mott, N. F. (1947), Fragmentation of Shell Cases, *Proc. Royal Soc.*, A189, 300–308, January.